Available online at www.sciencedirect.com
ScienceDirect
Pattern Recognition 41 (2008) 2461–2469
PATTERN RECOGNITION
THE JOURNAL OF THE PATTERN RECOGNITION SOCIETY
www.elsevier.com/locate/pr

# Chromaticity-based separation of reflection components in a single image

Hui-Liang Shen[a,*], Hong-Gang Zhang[a], Si-Jie Shao[b], John H. Xin[b]

[a]Department of Information and Electronic Engineering, Zhejiang University, Hangzhou 310027, China
[b]Institute of Textiles and Clothing, The Hong Kong Polytechnic University, Hong Kong, China

Received 30 May 2007; received in revised form 24 January 2008; accepted 28 January 2008

**Abstract**

The separation of diffuse and specular reflection components, or equivalently specularity removal, is required in the fields of computer vision, object recognition and image synthesis. This paper proposes a simple and effective method to separate reflections in a color image based on the error analysis of chromaticity and appropriate selection of body color for each pixel. By solving the least-squares problem of the dichromatic reflection model, reflection separation is implemented on a single pixel level, without requiring image segmentation and even local interactions between neighboring pixels. Experimental evaluation indicates that the proposed method is effective and can deal with a wide variety of images.
© 2008 Elsevier Ltd. All rights reserved.

*Keywords:* Reflection components separation; Diffuse reflection; Specular reflection; Chromaticity; Dichromatic reflection model; Image restoration

## 1. Introduction

For a wide variety of inhomogeneous materials, including plastic, wood, ceramic and other opaque nonconductors with uniform pigmentation, the reflection is the combination of diffuse reflection and specular reflection, which can be well described by the dichromatic reflection model introduced by Shafer [1]. The role of specular reflection is very important in the fields including computer vision [2,3], object recognition [4,5] and image content editing [6,7]. As many algorithms in computer vision and object recognition assume that the scene contains only diffuse reflection, they will become erroneous in the existence of specular reflection. As the specular reflection is relevant to the roughness of object surface, it should be first recovered and then incorporated in the simulation of new object appearances. With these regards, it is often desired to separate the diffuse and specular reflection components accurately from one or more images [8–12].

### 1.1. Previous work

Many methods for separating reflection components have been proposed in the literature. Nayar et al. [8] used a polarization filter to identify the highlights based on the fact that, for dielectric materials, the specular component is polarized while the diffuse component is not. The work of Tan et al. [9] was the first one that proposed the concept of specular-free (SF) image, which contains the identical geometry of the original image while eliminates the specular reflection components. Through the intensity logarithmic differentiation on both of the original and SF images, the pixels containing only diffuse reflections can be successfully localized. The specular components of highlight pixels are then removed in a two-pixel neighborhood region by employing an iterative framework. Tan et al. [10] also proposed another method for separating reflection components of uniformly colored surfaces based on the analysis of chromaticity and noise in the maximum chromaticity–intensity space.

Park and Lee [11] proposed a highlight inpainting method based on color line projection, by employing two images captured under different exposure times. Mallick et al. [12] proposed a unified framework to separate two reflection components from images and videos by using a partial differential equation approach. Their work also showed that different object surface appearances could be simulated by editing and recombining these two reflection components. Tan et al. [13] introduced an image inpainting technique for highlight removal without losing surface textures, by using the partially available information of diffuse reflections in the highlight areas.

* Corresponding author. Tel.: +86 571 87952501; fax: +86 571 87952116.
*E-mail addresses:* shenhl@zju.edu.cn (H.-L. Shen), tcxinjh@inet.polyu.edu.hk (J.H. Xin).

0031-3203/$30.00 © 2008 Elsevier Ltd. All rights reserved.
doi:10.1016/j.patcog.2008.01.026

### 1.2. Contributions of our method

It is noted that most of the previous works deal with the separation of reflection components by color projection or color shift in RGB space or a specified color space [9,11,13]. When the objects are not uniformly colored, preprocessing procedures such as image segmentation are needed before applying the method proposed in Ref. [10]. When there are multicolored objects or textures in the scenes, the local interactions between pixels must be considered in many methods [9,12,13], which makes the algorithm complicated to implement. Although the method introduced by Nayar et al. [8] can obtain accurate results, using an additional polarization filter seems impractical in many imaging circumstances.

In this study, we propose a simple and effective method to separate the diffuse and specular reflection components by the direct use of dichromatic reflection model [1]. It is known that the diffuse reflection represents the intrinsic properties of the object surfaces, while the color of the specular reflection is always the same to that of the illuminant [14]. Hereafter, the RGB vector (camera response) of the intrinsic material spectral reflectance is referred as body color, and the RGB vector of the spectral power distribution of the imaging illuminant is termed as illuminant color. The illuminant color can be simply acquired by imaging a white object surface. If this is not applicable, the illuminant color can be estimated using color constancy algorithms [15]. It is obvious that if the body color is known, the proportions of the diffuse and specular reflection components can be easily computed by solving the dichromatic equation under the least-squares criterion [6]. As image segmentation and other image operations are usually inappropriate to complex scenes, the proposed method estimates the body color for each pixel based on chromaticity analysis.

In the proposed method, a new SF image and a modified SF (MSF) image are introduced. The SF image is obtained by subtracting the minimum RGB value at each pixel position, and the MSF image is formed by adding a same scalar value for each pixel on the SF image. The noise analysis indicates that the MSF image is more robust than the SF image, and therefore the former is used to compute the chromaticity for each pixel. The approximate diffuse and specular candidates are decided according to the difference between the MSF and original images. Then, by iterative selection of body colors and calculation of chromaticity differences, the diffuse and specular reflection components are appropriately separated by the least-squares technique.

The rest of this paper is organized as follows. Section 2 presents the concept of the SF and MSF images, and their robustness of chromaticity with respect to imaging noise is analyzed statistically. Section 3 outlines the procedure for separating diffuse and specular reflections in a color image. Experimental results and discussion are provided in Section 4. Section 5 is the conclusion of this paper.

## 2. Specular-free images and chromaticity analysis

According to the dichromatic reflection model, the color $\mathbf{V}(p)$ of a pixel $p$ is the linear combination of diffuse reflection component with body color $\mathbf{V}_\mathrm{b}$ and specular reflection component with surface color $\mathbf{V}_\mathrm{s}$:

$$\mathbf{V}(p) = \alpha(p)\mathbf{V}_\mathrm{b} + \beta(p)\mathbf{V}_\mathrm{s} \tag{1}$$

where $\alpha(p)$ and $\beta(p)$ are the coefficients (or proportions) of the diffuse and specular reflection components, respectively. The illuminant color can be obtained by imaging a white object surface or estimated using color constancy algorithms. Then the color of each pixel is first normalized with respect to the illuminant color and then rescaled to the range 0–255 [10]. By this operation the surface color becomes pure white, or more precisely, $\mathbf{V}_\mathrm{s}=[255, 255, 255]^\mathrm{T}$, with the superscript T denoting vector transpose. It is obvious from Eq. (1) that, as the colors contain three components, i.e., red, green and blue, the two coefficients $\alpha(p)$ and $\beta(p)$ can be computed using least-squares, provided that the body color $\mathbf{V}_\mathrm{b}$ is available. The following subsections illustrate how the body color $\mathbf{V}_\mathrm{b}$ of each pixel can be decided by the chromaticity analysis of the MSF image.

### 2.1. SF and MSF images

The concept of SF image was first introduced by Tan et al. [9]. In their work, the SF image is obtained by setting the diffuse maximum chromaticity equal to a scalar value for all pixels, and computing the estimated specular components from the original colors. The geometry information of their SF image is the same to that of the original image, but the color information may be quite different [9]. Fig. 1(d) shows the SF image of a fish image using their method when the diffuse maximum chromaticity is set to 0.5.

As the most important purpose of SF image is to eliminate the specular reflection components, it can actually be produced in a very simple manner, i.e., by subtracting the minimum of the RGB components of the color $\mathbf{V}(p)$:

$$\begin{aligned} V_{\mathrm{sf},i}(p) &= V_i(p) - \min(V_1(p), V_2(p), V_3(p)) \\ &= V_i(p) - V_{\min}(p) \end{aligned} \tag{2}$$

where $V_i(p)$ is the $i$th element of color $\mathbf{V}(p)$, and $V_{\mathrm{sf},i}(p)$ is the $i$th element of the SF color $\mathbf{V}_\mathrm{sf}(p)$, and

$$\begin{aligned} V_{\min}(p) &= \min(V_1(p), V_2(p), V_3(p)) \\ &= \alpha(p)\min(V_{\mathrm{b},1}, V_{\mathrm{b},2}, V_{\mathrm{b},3}) + \beta(p)V_\mathrm{s} \\ &= \alpha(p)V_{\mathrm{b},\min} + \beta(p)V_\mathrm{s} \end{aligned} \tag{3}$$

where $V_{\mathrm{b},i}$ is the $i$th element of body color $\mathbf{V}_\mathrm{b}$, $V_{\mathrm{b},\min} = \min_i(V_{\mathrm{b},i})$ and $V_\mathrm{s}$ is the component of color $\mathbf{V}_\mathrm{s}$. Note that the subscript $i$ of $V_\mathrm{s}$ is omitted as the surface color $\mathbf{V}_\mathrm{s}$ is pure white after the normalization with respect to illuminant color. By combining Eqs. (2) and (3), the SF color can be rewritten as

$$V_{\mathrm{sf},i}(p) = \alpha(p)(V_{\mathrm{b},i} - V_{\mathrm{b},\min}) \tag{4}$$

It is clear from Eq. (4) that the specular component is eliminated while the geometry information is reserved in the SF image.

It can be observed from Eq. (4) that, as $V_{\mathrm{b},\min} = \min_i(V_{\mathrm{b},i})$, at least one element of the vector $\mathbf{V}_\mathrm{sf}(p)$ is 0, and hence the color appearance of the SF image is always darker than that of the original image.

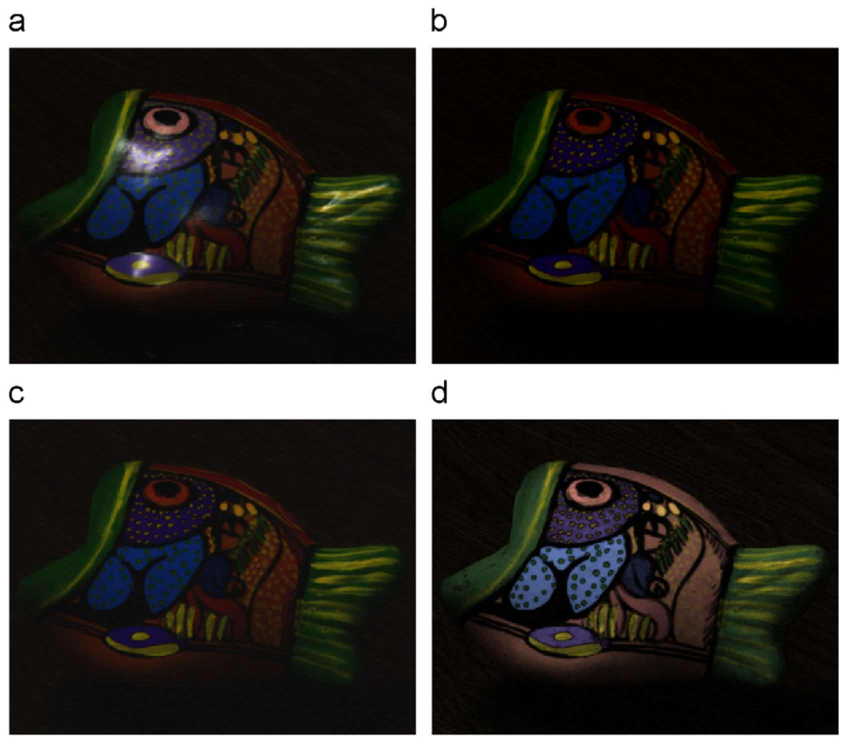


Fig. 1. (a) Original fish image, (b) SF image of the proposed method, (c) MSF image, (d) SF image by Tan's method.

As will be seen, the chromaticity of the SF image is unstable when the other two elements of $\mathbf{V}_{\rm sf}(p)$ are also small. With these regards, we propose to calculate an MSF image by adding a scalar value on SF color:

$$V_{{\rm msf},i}(p) = V_{{\rm sf},i}(p) + \overline{V}_{\rm min} \tag{5}$$

where $V_{{\rm msf},i}(p)$ is the $i$th element of the MSF color vector $\mathbf{V}_{\rm msf}(p)$, and $\overline{V}_{\rm min}$ is the mean of $V_{\rm min}(p)$ for all the pixels in the image:

$$\overline{V}_{\rm min} = \frac{\sum_p V_{\rm min}(p)}{\#\text{pixels}} \tag{6}$$

Fig. 1 shows that, compared with the SF image, the color appearance of the MSF image is closer to that of the original image.

### 2.2. Error analysis of chromaticity

The chromaticity of the SF and MSF images can be computed according to Eqs. (7) and (8), respectively:

$$c_{{\rm sf},i}(p) = \frac{V_{{\rm sf},i}(p)}{\sum_i V_{{\rm sf},i}(p)} = \frac{V_{{\rm b},i} - V_{\rm b,min}}{\sum_i (V_{{\rm b},i} - V_{\rm b,min})} \tag{7}$$

$$\begin{aligned} c_{{\rm msf},i}(p) &= \frac{V_{{\rm msf},i}(p)}{\sum_i V_{{\rm msf},i}(p)} = \frac{V_{{\rm sf},i}(p) + \overline{V}_{\rm min}}{\sum_i V_{{\rm sf},i}(p) + 3\overline{V}_{\rm min}} \\ &= \frac{\alpha(p)(V_{{\rm b},i} - V_{\rm b,min}) + \overline{V}_{\rm min}}{\alpha(p)\sum_i (V_{{\rm b},i} - V_{\rm b,min}) + 3\overline{V}_{\rm min}} \end{aligned} \tag{8}$$

The chromaticity $c_{{\rm sf},i}(p)$ of the SF image is invariant to shape geometry, but will be unstable for the dark or neutral color when the denominator $V_{{\rm b},i} - V_{\rm b,min}$ is small. The chromaticity $c_{{\rm msf},i}(p)$ depends upon $\alpha(p)$, and it still contains partial geometry information of the object surface. Due to the additional term $3\overline{V}_{\rm min}$ in the denominator, $c_{{\rm msf},i}(p)$ should be more robust to noise influence than $c_{{\rm sf},i}(p)$ when the term $\sum_i (V_{{\rm b},i} - V_{\rm b,min})$ is close to zero. When $\overline{V}_{\rm min}$ is significantly smaller than $(V_{{\rm b},i} - V_{\rm b,min})$, $c_{{\rm msf},i}(p)$ will be very close to $c_{{\rm sf},i}(p)$. The chromaticity of the SF and MSF images are shown in Fig. 2. It is found that the chromaticities of different regions of the MSF image are not as distinct as those of the SF image. As expected, they are insensitive to noise.

As the robustness of chromaticity is fundamental to our proposed method, it is worthwhile to investigate the influence of noise more deeply. Let the measurement of a random quantity $u$ be given as

$$\hat{u} = \overline{u} + \sigma_u \tag{9}$$

where $\overline{u}$ is the mean of the measurements that best estimates the ideal quantity $u$, and $\sigma_u$ is the uncertainty of the measurements. $\sigma_u$ can be represented by the standard deviation of the measurements. Suppose the quantities $u, \ldots, w$ are measured with uncertainty $\sigma_u, \ldots, \sigma_w$ and a function $f(u, \ldots, w)$ is computed from these quantities, then the uncertainty of the function $f(u, \ldots, w)$ can be computed as [16]:

$$\sigma_f = \left[ \left( \frac{\partial f}{\partial u} \sigma_u \right)^2 + \cdots + \left( \frac{\partial f}{\partial w} \sigma_w \right)^2 \right]^{1/2} \tag{10}$$

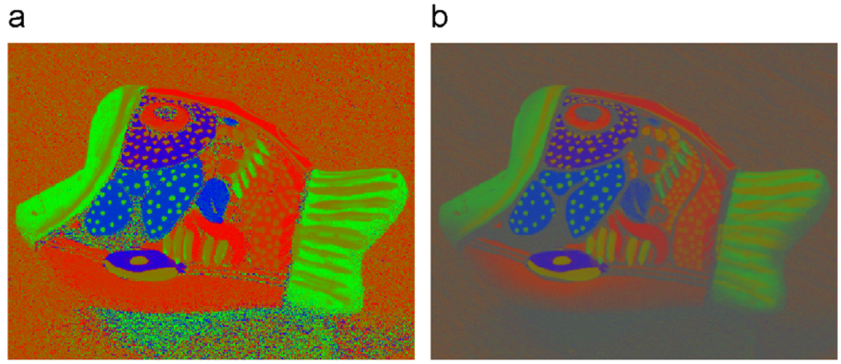

Fig. 2. Chromaticity of the SF image (a) and MSF image (b).

Suppose the uncertainty of $V_{\mathrm{sf},i}(p)$ is $\sigma_{\mathrm{sf},i}(p)$, the uncertainty of chromaticity $c_{\mathrm{sf},1}(p)$ can be computed by substituting Eq. (7) into Eq. (10):

$$\sigma_{c_{\mathrm{sf},1}}(p) = \frac{[(V_{\mathrm{sf},2}(p)+V_{\mathrm{sf},3}(p))^2\sigma^2_{\mathrm{sf},1}(p)+V^2_{\mathrm{sf},1}(p)(\sigma^2_{\mathrm{sf},2}(p)+\sigma^2_{\mathrm{sf},3}(p))]^{1/2}}{(V_{\mathrm{sf},1}(p)+V_{\mathrm{sf},2}(p)+V_{\mathrm{sf},3}(p))^2}. \tag{11}$$

The uncertainties $\sigma_{c_{\mathrm{sf},2}}(p)$ and $\sigma_{c_{\mathrm{sf},3}}(p)$ can be computed in a similar way. Eq. (11) indicates that when $V_{\mathrm{sf},i}(p)$ is close to zero, the uncertainty of the chromaticity $c_{\mathrm{sf},i}(p)$ will be magnified.

If the uncertainty of $V_{\mathrm{msf},i}(p)$ is also $\sigma_{\mathrm{sf},i}(p)$, the uncertainty of $c_{\mathrm{msf},1}(p)$ is computed as

$$\begin{aligned}\sigma_{c_{\mathrm{msf},1}}(p) &= \frac{[(V_{\mathrm{msf},2}(p)+V_{\mathrm{msf},3}(p))^2\sigma^2_{\mathrm{sf},1}(p)+V^2_{\mathrm{msf},1}(p)(\sigma^2_{\mathrm{sf},2}(p)+\sigma^2_{\mathrm{sf},3}(p))]^{1/2}}{(V_{\mathrm{msf},1}(p)+V_{\mathrm{msf},2}(p)+V_{\mathrm{msf},3}(p))^2}\\ &= \frac{[(V_{\mathrm{sf},2}(p)+V_{\mathrm{sf},3}(p)+2\overline{V}_{\min})^2\sigma^2_{\mathrm{sf},1}(p)+(V_{\mathrm{sf},1}(p)+\overline{V}_{\min})^2(\sigma^2_{\mathrm{sf},2}(p)+\sigma^2_{\mathrm{sf},3}(p))]^{1/2}}{(V_{\mathrm{sf},1}(p)+V_{\mathrm{sf},2}(p)+V_{\mathrm{sf},3}(p)+3\overline{V}_{\min})^2}.\end{aligned} \tag{12}$$

The uncertainties $\sigma_{c_{\mathrm{msf},2}}(p)$ and $\sigma_{c_{\mathrm{msf},3}}(p)$ can also be computed in a similar way. As there is a term $\overline{V}_{\min}$ in the denominator in Eq. (12), the uncertainty of the chromaticity $c_{\mathrm{msf},i}(p)$ is always not large.

It is of interest to investigate the magnitude of noise influence on chromaticity calculation by data simulation. For simplicity, we only consider the dark current noise of the camera and suppose it is intensity independent and normally distributed with zero mean. Suppose $V_{\mathrm{sf},1}(p)=10+n(0,\sigma)$, $V_{\mathrm{sf},2}(p)=10+n(0,\sigma)$, $V_{\mathrm{sf},3}(p)=20+n(0,\sigma)$ and $\overline{V}_{\min}=20$, where $n(0,\sigma)$ denotes the additional Gaussian noise with variance $\sigma=3$. Figs. 3(a) and (b) show the distributions of chromaticity $c_{\mathrm{sf},i}(p)$ and $c_{\mathrm{msf},i}(p)$ with respect to different geometry coefficient $\alpha(p)$. The red curves in Fig. 3 are the chromaticity distributions without consideration of noise. The standard deviation of the chromaticity error of $c_{\mathrm{sf},i}(p)$ and $c_{\mathrm{msf},i}(p)$ is 0.025 and 0.007, respectively, which means that the uncertainty of $\sigma_{c_{\mathrm{sf},i}}(p)$ is 3.6 times larger than that of $\sigma_{c_{\mathrm{msf},i}}(p)$. With this regard, the chromaticity $c_{\mathrm{msf},i}(p)$ is used in the proposed method for reflection separation, as discussed in the following.

## 3. Separation of reflection components

In order to decide the body color $\mathbf{V}_\mathrm{b}$ for each pixel, we first classify all pixels in the image into two sets. The first set is a collection of candidates with sole diffuse reflection, while the second set is a collection of candidates with combined reflections (diffuse and specular reflections). The candidate classification is implemented on the single pixel level, based on the difference between the MSF and original images:

$$\text{candidate} = \begin{cases}\text{diffuse} & \text{if } V_i(p)-V_{\mathrm{msf},i}(p) < th1 \text{ for all } i\\ \text{combined} & \text{otherwise}\end{cases} \tag{13}$$

It is usually impossible to classify all the pixels in an image into two reflection sets exactly by using only a single threshold $th1$. Fortunately, as the purpose is to decide the body color, an approximate candidate classification will be adequate. The criterion of $th1$ selection is that the pixels satisfying $V_i(p)-V_{\mathrm{msf},i}(p)<th1$ must contain sole diffuse reflection, while those satisfying $V_i(p)-V_{\mathrm{msf},i}(p)\geqslant th1$ can contain either sole diffuse reflection or combined reflections. Our investigation indicates that $th1=\overline{V}_{\min}$ is suitable to all images (more than 25) used in this study. Fig. 4 shows the diffuse and combined candidates of the fish image.

The reflection separation is implemented in an iterative manner. In each iteration, an appropriate diffuse candidate is treated as the body color $\mathbf{V}_\mathrm{b}$, and then the coefficients $\alpha(p)$ and $\beta(p)$ of the pixels with chromaticity close to that candidate are computed. As there is always noise in an image, two concerns are specially considered: (1) the body color is always the diffuse candidate with the largest intensity, and (2) the reflection separation is applied on both diffuse and combined candidates such that the separated diffuse components $\mathbf{V}_{\mathrm{df}}$ is error-free while the specular components $\mathbf{V}_{\mathrm{sp}}$ may contains imaging noise.

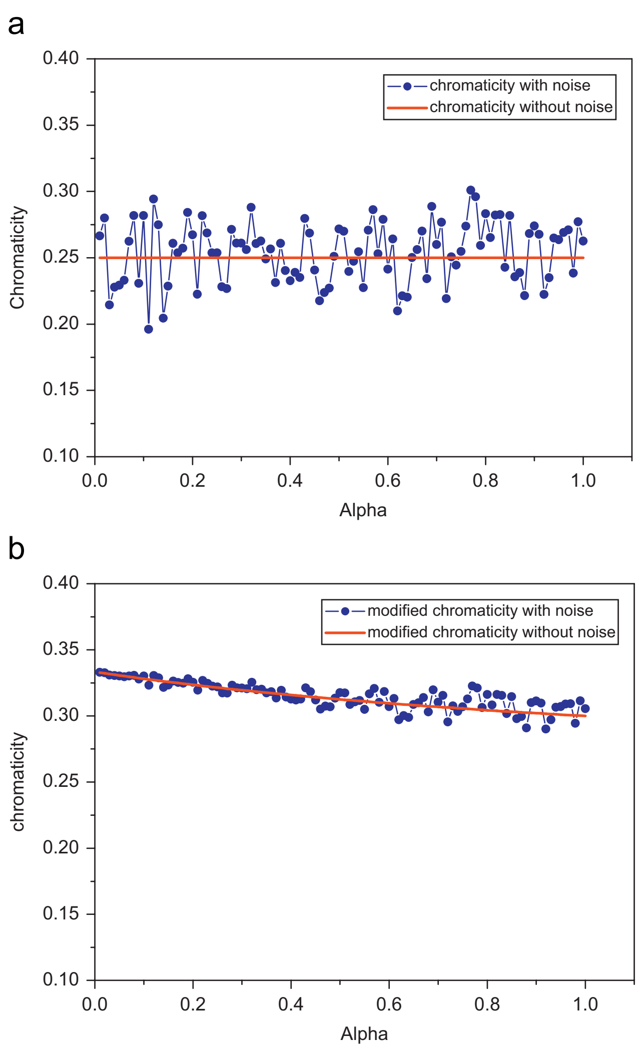


Fig. 3. Distribution of chromaticity with respect to different $\alpha$ values when influenced by noise: (a) chromaticity of the SF image; (b) chromaticity of the MSF image.

Refer to Eqs. (17), (18), (22), (23) for details. The procedure of reflection separation is as follows:

- Step 1: Iterate while there are any unprocessed diffuse candidates
  Find the pixel $p$ with the largest $V_{\max}(p)$ $(=\max_i V_i(p))$ among those unprocessed diffuse candidates, and set the color of $p$ as body color $\mathbf{V}_{\mathrm{b}}(p)$.
  For each unprocessed pixel $q$ (can be either diffuse or combined candidate) satisfying

$$\sum_i |c_{\mathrm{msf},i}(q) - c_{\mathrm{msf},i}(p)| \leqslant th2 \tag{14}$$

where $th2$ is a chromaticity threshold, compute its reflection coefficients under the least-squares criterion:

$$\begin{bmatrix} \alpha(q) \\ \beta(q) \end{bmatrix} = [\mathbf{V}_{\mathrm{b}}(p) \ \ \mathbf{V}_{\mathrm{s}}]^{-}\mathbf{V}(q) \tag{15}$$

where the superscript "–" denotes pseudo-inverse. If $\beta(q) < 0$, recompute $\alpha(q)$ as

$$\alpha(q) = \mathbf{V}_{\mathrm{b}}(p)^{-}\mathbf{V}(q) \tag{16}$$

Eq. (16) is built on the fact that specular reflection is generally nonnegative. After obtaining the diffuse coefficient $\alpha(q)$

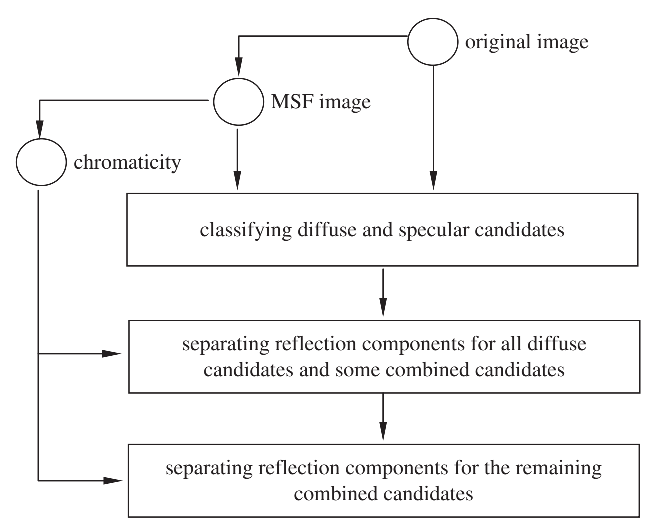


Fig. 5. Flowchart of the proposed method.

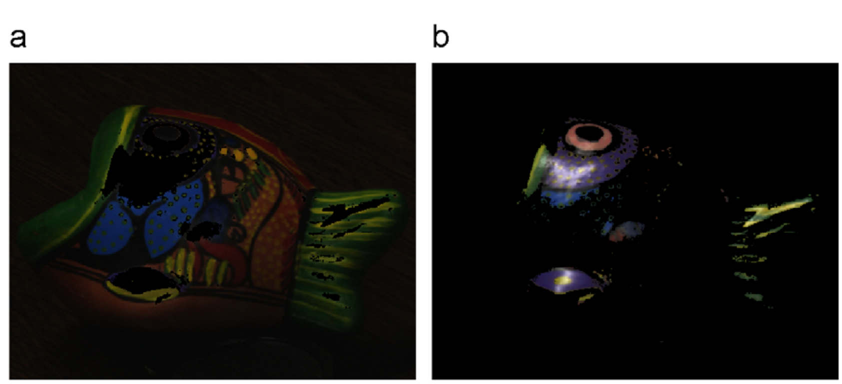


Fig. 4. (a) Diffuse candidates and (b) combined candidates.

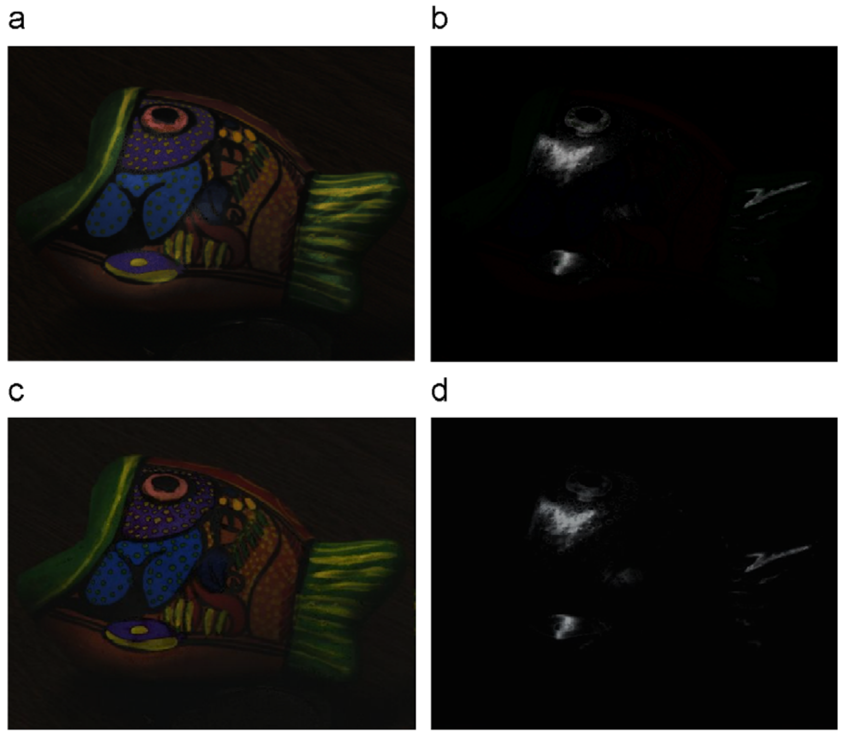


Fig. 6. (a) and (b) The diffuse and specular components by the proposed method, respectively. (c) and (d) The diffuse and specular components by Tan's method, respectively.

according to Eq. (15) or (16), we compute the diffuse reflection component $\mathbf{V}_{\mathrm{df}}(q)$ and specular reflection component $\mathbf{V}_{\mathrm{sp}}(q)$:

$$\mathbf{V}_{\mathrm{df}}(q) = \alpha(q)\mathbf{V}_{\mathrm{b}}(p) \tag{17}$$

$$\mathbf{V}_{\mathrm{sp}}(q) = \mathbf{V}(q) - \alpha(q)\mathbf{V}_{\mathrm{b}}(p) \tag{18}$$

and finally the pixel $q$ is labeled as processed. It is noted that $\mathbf{V}_{\mathrm{df}}(q)$ is error-free, while $\mathbf{V}_{\mathrm{sp}}(q)$ may incorporate the influence of noise.

- Step 2: Iterate while there are any unprocessed combined candidates
  Take an unprocessed combined candidate $r$ in the sequential manner, and find the already processed pixel $p^*$ whose chromaticity is closest to that of pixel $r$

$$p^* = \operatorname*{argmin}_{p} |c_{\mathrm{msf}}(p) - c_{\mathrm{msf}}(r)| \tag{19}$$

For each unprocessed pixel $q$ (combined candidate) satisfying

$$\sum_i |c_{\mathrm{msf},i}(q) - c_{\mathrm{msf},i}(p^*)| \leqslant th2 \tag{20}$$

compute its reflection coefficients according to

$$\begin{bmatrix} \alpha(q) \\ \beta(q) \end{bmatrix} = [\mathbf{V}_{\mathrm{df}}(p^*)\ \ \mathbf{V}_{\mathrm{s}}]^{-}\mathbf{V}(q) \tag{21}$$

Note that $\mathbf{V}_{\mathrm{df}}(p^*)$ is used instead of $\mathbf{V}(p^*)$ in Eq. (21). Then, the diffuse and specular reflection components become

$$\mathbf{V}_{\mathrm{df}}(q) = \alpha(q)\mathbf{V}_{\mathrm{df}}(p^*) \tag{22}$$

$$\mathbf{V}_{\mathrm{sp}}(q) = \mathbf{V}(q) - \alpha(q)\mathbf{V}_{\mathrm{df}}(p^*) \tag{23}$$

and finally the pixel $q$ is labeled as processed.

It can be noticed that, in step 1, all diffuse candidates and some combined candidates are processed, while in step 2, the remaining combined candidates are processed. It is noted that the pixel $p^*$ in Eq. (19) need not be the one with maximum intensity, as its diffuse reflection component $\mathbf{V}_{\mathrm{df}}(p^*)$ is error-free after the processing in step 1. The chromaticity threshold $th2 = 0.05$ is suitable in this study.

## 4. Experiment results

For the purpose of easy understanding, the flowchart of the proposed method is illustrated in Fig. 5. The MSF image is computed by subtracting the minimum intensity and adding a scalar value so that its chromaticity becomes stable. All pixels are classified into diffuse and combined candidates by thresholding the difference between the MSF image and the original image. The separation of reflection components is implemented in an iterative manner, by selecting appropriate body color and computing chromaticity difference for each pixel. In the first stage, the reflection separation is applied on all diffuse candidates and some combined candidates, and in the second stage, it is applied on the remaining combined candidates.

The proposed method is completed and evaluated under the environment of Microsoft Windows XP® and Visual C++ 6.0, on a PC with Intel® Core™ 2 CPU and 2 GHz memory.

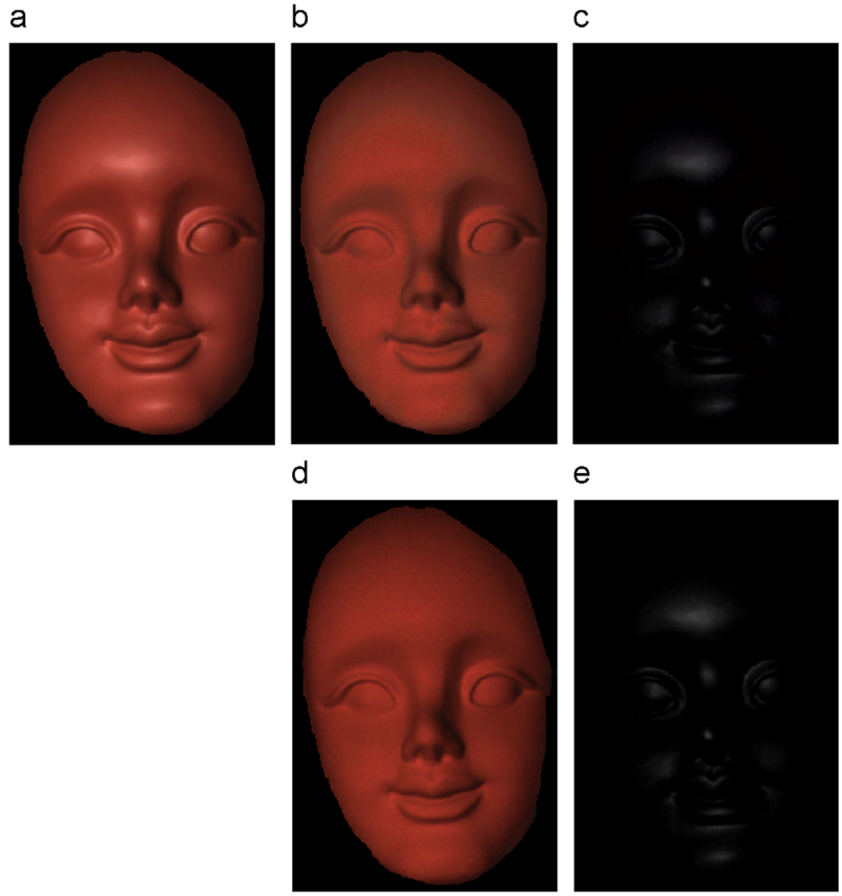


Fig. 7. (a) Original boy image. (b) and (c) The diffuse and specular components by the proposed method, respectively. (d) and (e) The diffuse and specular components by Tan's method, respectively.

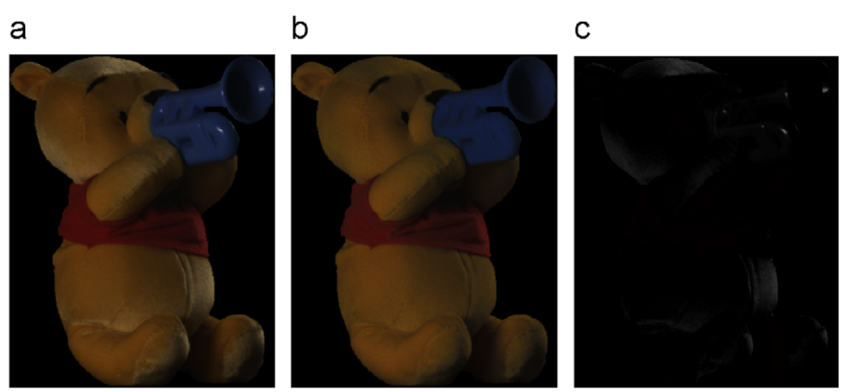


Fig. 8. (a) Original bear image, (b) diffuse component, (c) specular component.

More than 25 images were used to evaluate the effectiveness of the proposed method. For typical images with about $380 \times 360$ pixels, the average running time of the proposed method is around 0.6 s, while that of Tan's method [10] is about 20 s. The original fish image in Fig. 6 contains textures and many regions. The separated reflection components of the fish image are similar to those obtained by Tan's method. Fig. 7 shows the experimental results of a uniformly colored boy image. Again, the performance of the proposed method is close to Tan's method. Fig. 8 shows the separation results of a textile bear with a horn. The highlights on the two different materials, i.e. textile and plastic, are successfully detected and appropriately separated. Fig. 9 indicated that the proposed method can also be applied on human face. The original image in Fig. 10 contains many highlights in different positions of the three toys, which are also handled by the proposed method successfully.

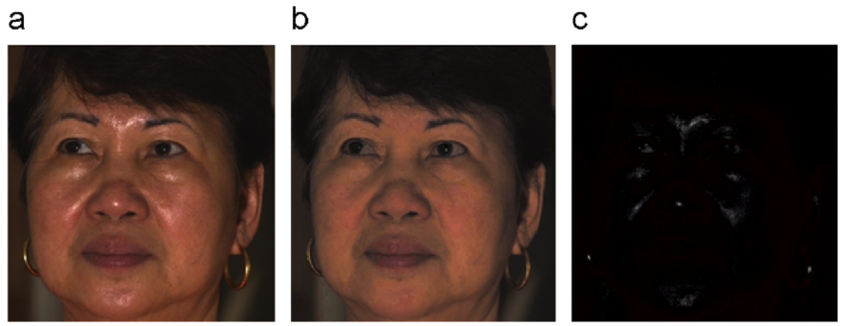


Fig. 9. (a) Original lady image, (b) diffuse component, (c) specular component.

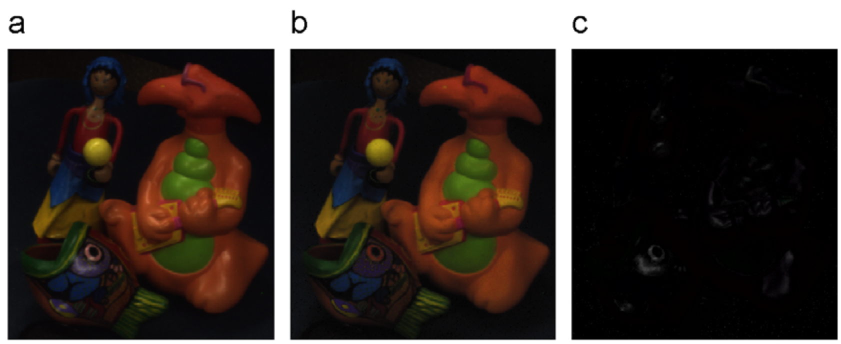


Fig. 10. (a) Original toys image, (b) diffuse component, (c) specular component.

## 5. Conclusions

We have proposed a method for the separation of diffuse and specular reflection components in a color image. The advantages and contributions of the proposed method are that (1) it does not require image segmentation and even local interaction of neighboring pixels, and (2) the reflection component separation is very easily implemented by solving the dichromatic equation using the least-squares technique. The experimental results showed that the performance of the proposed method is promising and can deal with various kinds of images.

## Acknowledgments

We thank R.T. Tan for providing some images used in this paper. This work was supported by the NSF of China under Grant no. 60602027.

## References

[1] S.A. Shafer, Using color to separate reflection components, Color Res. Appl. 10 (1985) 210–218.

[2] S. Barsky, M. Petrou, The 4-source photometric stereo technique for three-dimensional surfaces in the presence of highlights and shadows, IEEE Trans. Pattern Anal. Mach. Intell. 25 (2003) 1239–1252.

[3] H.C. Lee, E.J. Breneman, C.P. Schulte, Modeling light reflection for computer vision, IEEE Trans. Pattern Anal. Mach. Intell. 12 (1990) 402–409.

[4] S. Tominaga, Surface identification using the dichromatic reflection model, IEEE Trans. Pattern Anal. Mach. Intell. 13 (1991) 658–670.

[5] T. Gevers, A.W.M. Smeulders, Color-based object recognition, Pattern Recognition 32 (1999) 453–464.

[6] H.L. Shen, J.H. Xin, Analysis and synthesis of multicolored objects in a single image, Opt. Lett. 30 (2005) 2378–2380.

[7] S. Tominaga, N. Tanaka, Refractive index estimation and color image rendering, Patter Recognition Lett. 24 (2003) 1703–1713.

[8] S.K. Nayar, X.S. Fang, T. Boult, Separation of reflection components using color and polarization, Int. J. Comput. Vision 21 (1997) 163–186.

[9] R.T. Tan, K. Nishino, K. Ikeuchi, Separating reflection components based on chromaticity and noise analysis, IEEE Trans. Pattern Anal. Mach. Intell. 26 (2004) 1373–1379.

[10] R.T. Tan, K. Ikeuchi, Separating reflection components of textured surfaces using a single image, IEEE Trans. Pattern Anal. Mach. Intell. 27 (2005) 178–193.

[11] J.W. Park, K.H. Lee, Inpainting highlights using color line projection, IEICE Trans. Inform. Syst. E90D (2007) 250–257.

[12] S.P. Mallick, T. Zickler, P.N. Belhumeur, D.J. Kriegman, Specularity removal in images and videos: a PDE approach, in: A. Leonardis, H. Bischof, A. Pinz (Eds.), Lecture Notes in Computer Science, vol. 3951, Springer, Berlin, 2006, pp. 550–563.

[13] P. Tan, S. Lin, L. Quan, H.Y. Shum, Highlight removal by illumination-constrained inpainting, in: Proceedings of the Ninth IEEE International Conference on Computer Vision, Nice, France, 2003, pp. 164–169.

[14] H.C. Lee, D.J. Breneman, C.O. Schulte, Modeling light reflection for computer color vision, IEEE Trans. Pattern Anal. Mach. Intell. 12 (1990) 402–409.

[15] H.C. Lee, Method for computing the scene-illuminant chromaticity from specular highlights, J. Opt. Soc. Am. A 3 (1986) 1694–1699.

[16] T. Gevers, H. Stokman, Classifying color edges in video into shadow-geometry, highlight or material transitions, IEEE Trans. Multimedia 5 (2003) 237–243.

**About the Author**—HUI-LIANG SHEN received his Ph.D. degree in electronic engineering from Zhejiang University, China, in 2002. He has been a researcher associate and post-doctorial fellow in the Institute of Textiles and Clothing, The Hong Kong Polytechnic University, from 2001 to 2005. He joined Department of Information and Electronic Engineering, Zhejiang University, in 2005, and is currently an associate professor. His research interests are image processing, computer vision and color imaging.

**About the Author**—HONG-GANG ZHANG received his B.E. degree in electronic engineering from Zhejiang University, China, in 2006. He is currently pursuing his M.E. degree. His research interest is image processing.

**About the Author**—SI-JIE SHAO received his Ph.D. degree from The Hong Kong Polytechnic University in 2006, and is currently a research fellow in the University. He is interested in image processing and color imaging.

**About the Author**—JOHN H. XIN is a key researcher at the Institute of Textiles and Clothing, The Hong Kong Polytechnic University. His research interests range from color quality control, color difference, color imaging, to color communication. Professor Xin graduated from the University of Leeds, UK, with a Ph.D. in textile chemistry. He is a charted colorist of the Society of Dyers and Colorists, UK, and editor of the journal, *Coloration Technology*. He is also an editor of the *Journal of the Textile Institute*.